

# Fracture Toughness of Titanium Foam Using Finite Element Crushable Foam Model

Talal S. Mandourah \*

Mechanical Engineering Department, College of Engineering and Islamic Architecture,  
Umm Al-Qura University, Makkah, KSA

\*Corresponding author: [tmandourah@gmail.com](mailto:tmandourah@gmail.com)

Received October 12, 2018; Revised November 15, 2018; Accepted November 28, 2018

**Abstract** Titanium foam is considering an important competitive in bio-system applications, this is due to its compatibility as well as fascination. Getting good sufficient data about fracture and mechanical properties are needed demand for scientific and Engineering works in the field of biomaterial and bio-system. Fracture toughness is measured numerically using J-integral finite element method based on crushable foam model. Three-point single notch bending specimen is used for the foam of 62.5 %, and 65 % porosity to measured surface release energy  $G_{IC}$ . this test is considered a stander test for linear material. it is found to be (2.3), and (1.36)  $\text{kJ/m}^2$ , for 62.5% and 65 % porosity respectively. this is usually used in human implants. The measured  $G_{IC}$  is acceptable compared with that experimentally measured in other published paper.

**Keywords:** titanium foam, J-integral, porous material, crushable foam model

**Cite This Article:** Talal S. Mandourah, "Fracture Toughness of Titanium Foam Using Finite Element Crushable Foam Model." *American Journal of Mechanical Engineering*, vol. 6, no. 3 (2018): 127-131. doi: 10.12691/ajme-6-3-5.

## 1. Introduction

Nowadays metal foam has an attractive and competitive role in many applications such as in aircraft, shock absorber, structural components, sound and damper and in bio-systems implants and heat exchangers [1,2,3]. The foam superior distinguished properties such as high specific stiffness, low density, and high specific strength put it in the front role of bio-material material and give its important [4,5].

Titanium foam is one of most famous metal which play dominated role in biomedical implants where biocompatibility is a great demand. This is due to its high increase of interface coefficient of friction with between bones. While the titanium foam has the advantage of reducing the stress shield effect by varying porosities [5,6]. Finite element modeling implements in designing the dental locations, measured stress which may be subjected and stop on the defects may face the implant before it inserts in the human mandibular [7-11].

Tanwongwan and Carmai [12] implement crushable finite element model to obtain both compressive and flexural strength of titanium foams with different densities, the model gave acceptable results but not give complete information about plasticity behaviors.

Korim et al [13] measured both compressive and flexural strength and stiffness using finite element analysis based on crushable damage model and gave a complete description for plasticity. The results were in good and acceptable.

Many other models [14-17] work on either metal foam simulation using finite element method or titanium or even aluminum foams.

The main goal of the present study is measure fracture release energy  $G_{IC}$  of titanium foam for single edge notch three-point test specimen using crushable foam model implemented in finite element subroutine. The model description is completely detailed in this paper.

The paper is structured as follows: firstly, the crushable damage model of foam material will be outlines, Secondary, finite element domain with problems, boundary conditions and mesh domain are explained. Finally, the model results and conclusion are summarized.

### 1.1. Mechanical Behaviors of Metal Foams

The foam material is distinguished by its microstructure other than solid material. Spongy microstructure in foam presented by pores or cells. At Microstructure level, metal foam characterized by relative density, cell shape, cell topology and cell size [17,18,19]. The mechanical response affects by the internal microstructure, the compressive behaviors of such metal give three regions; linear elastic zone, a stress plateau zone, and finally the failure zone. Metal foam can deform up to large strain before full densification occurs [20-30].

### 1.2. Elastic and Crushable Model

The constative law for titanium foam is isotropic elastic combined by crushable foam hardening plasticity laws. the

elastic isotropic can state using the following stress-strain tensor [31].

$$\begin{Bmatrix} \varepsilon_{11} \\ \varepsilon_{22} \\ \varepsilon_{33} \\ \varepsilon_{12} \\ \varepsilon_{13} \\ \varepsilon_{23} \end{Bmatrix} = \begin{bmatrix} 1/E & -\nu/E & -\nu/E & 0 & 0 & 0 \\ -\nu/E & 1/E & -\nu/E & 0 & 0 & 0 \\ -\nu/E & -\nu/E & 1/E & 0 & 0 & 0 \\ 0 & 0 & 0 & 1/G & 0 & 0 \\ 0 & 0 & 0 & 0 & 1/G & 0 \\ 0 & 0 & 0 & 0 & 0 & 1/G \end{bmatrix} \begin{Bmatrix} \sigma_{11} \\ \sigma_{22} \\ \sigma_{33} \\ \sigma_{12} \\ \sigma_{13} \\ \sigma_{23} \end{Bmatrix}$$

The elastic properties are completely defined by giving Young's modulus  $E$ , and the Poisson's ratio  $\nu$ . The shear modulus  $G$  can be expressed in terms of  $E$  and  $\nu$  as

$$G = \frac{E}{2(1+\nu)} \tag{1}$$

The crushable foam model (see Figure 1) is useful in prediction plasticity foam shape under uniaxial loading compression or tension or more even tension.

The  $p$ - $q$  stress plane for crushable foam model is an ellipse of its center at the origin [21].

$$F = \sqrt{q^2 + \alpha^2 p^2} - B \tag{2}$$

Where  $F$  is a yield surface for the isotropic hardening model,  $p$  is the pressure stress,  $q$  is the Mises stress and  $B$  is the size of the (vertical)  $q$ -axis of the yield ellipse that obtained from equation (3)

$$B = \alpha p_c = \sigma_c \sqrt{1 + \left(\frac{\alpha}{3}\right)^2} \tag{3}$$

Where  $\alpha$  is the shape factor of the yield ellipse that defines the relative magnitude of the axes,  $p_c$  is the yield stress in hydrostatic compression, and  $\sigma_c$  is the absolute value of the yield stress in uniaxial compression, and  $\alpha$  is the shape factor that can be computed using the initial yield stress in uniaxial compression is given from

$$\alpha = \frac{3k}{\sqrt{9-k^2}} \tag{4}$$

The flow potential for the isotropic hardening model is chosen as  $v_p$

$$G = \sqrt{q^2 + \beta^2 p^2} \tag{5}$$

$$\beta = \frac{3}{\sqrt{2}} \sqrt{\frac{1-2\nu_p}{1+\nu_p}} \tag{6}$$

Where  $\nu_p$  is the plastic Poisson's ratio given by

$$\nu_p = \frac{3-k^2}{6} \tag{7}$$

The relative density  $p_r$  is assumed to linearly proportional to the percent of porosity according to Imwinkelried [14] and is illustrated in Figure 2.

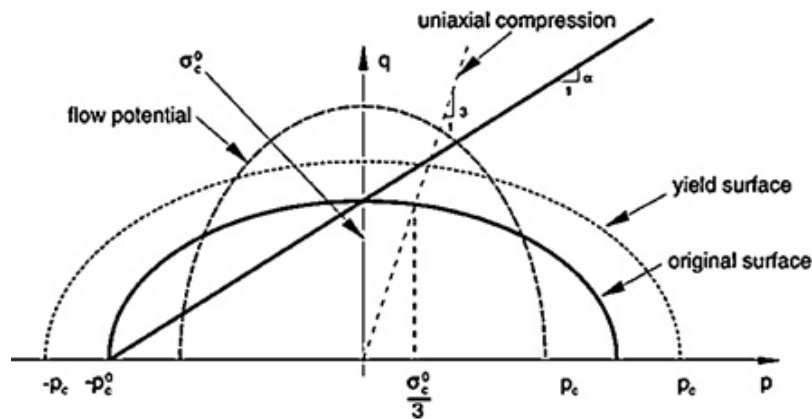


Figure 1. Crushable foam model with isotropic hardening: yield surface and flow potential in the  $p$ - $q$  stress plane [32]

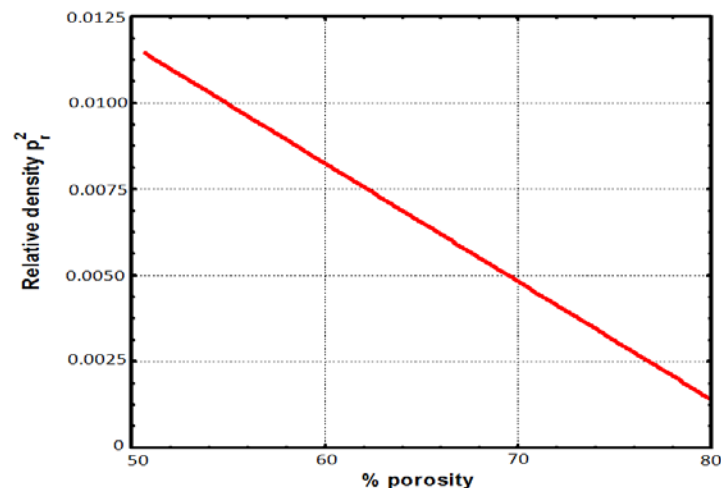


Figure 2. Relation between porosity and relative density

### 1.3. The Single Notch Three-point Bending Domain

The single notch three-point bending test of Ti-foam is simulated with the material module listed in Table 1. Finite element domain of three dimensional of the single notches three-point bending test is constructed as shown in Figure 3. The upper movable roller is loaded by 1mm displacement while the lower rollers are fixed. C3D8R (5238 elements): An 8-node linear brick, reduced integration, hourglass controls are used. The friction coefficient between the contact surfaces is set to be 0.5. The mechanical properties of Ti-foam specimen for three-point bending test are taken from crushable model equations, which are listed in Table 1. Figure 4 illustrates the mesh domain of three-point bending test while Figure 5 shows the Boundary condition of the three-point bending test and Interaction module between supporting and load rollers is shown in Figure 6.

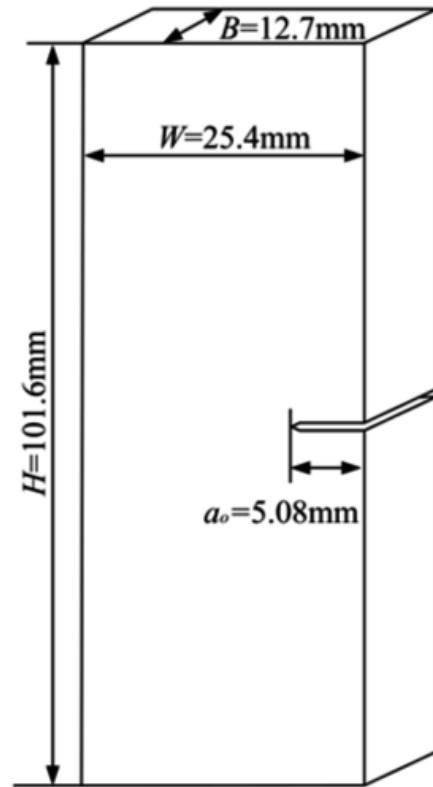


Figure 3. Single edge three-point bending specimen

Table 1. Mechanical properties of Ti-foam specimen with porosity (62.5%, 65%) for three-point bending

	Porous 62.5%	Porous 65%
Young's modulus, E (GPa)	9.9	8.71
Yield stress $\sigma$	70	55.61
Poisson's ratio, $\nu$	0.33	0.3
Compression yield stress ratio, k	0.98	0.98
Plastic Poisson's ratio, $\nu_p$	0.34	0.34

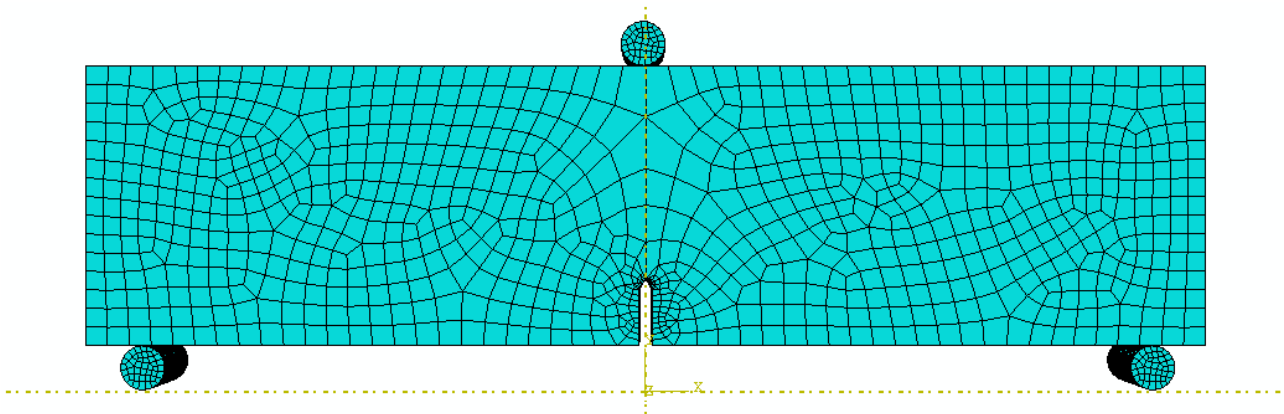


Figure 4. FE mesh domain of C3D8R (5238 elements)

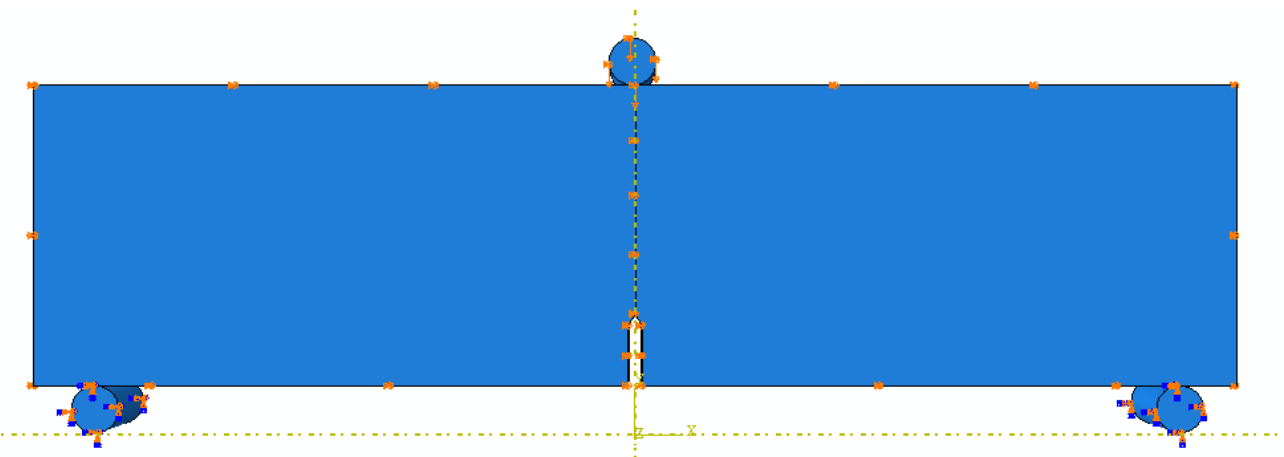


Figure 5. Boundary conditions of three-point single notch bending

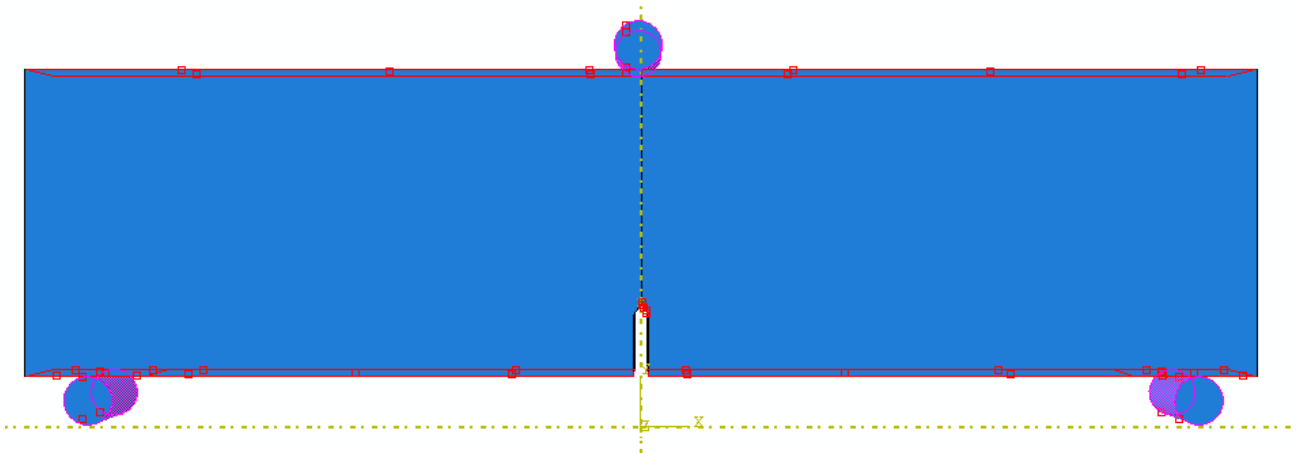


Figure 6. Boundary conditions of three-point single notch bending

## 2. Result and Discussion

Typical bending load-displacement curves for the three-point single notch bending tests are shown in Figure 7. The bending stress strongly depends on the porosity of the titanium foam. It is illustrated that as porosity increase flexural strength decrease this is due to decrease of strength with the porosity increment. The stress distribution and the failure modes are shown in the contour image, which is shown in Figure 8. It is clear that stress is very high at upper and lower surfaces at interfaces between upper and lower machine platen. The value of J-integral is measured as nearly) (2.3), and (1.36)  $\text{kJ/m}^2$ , for 62.5% and 65 % porosity respectively titanium foam (see Figure 9).

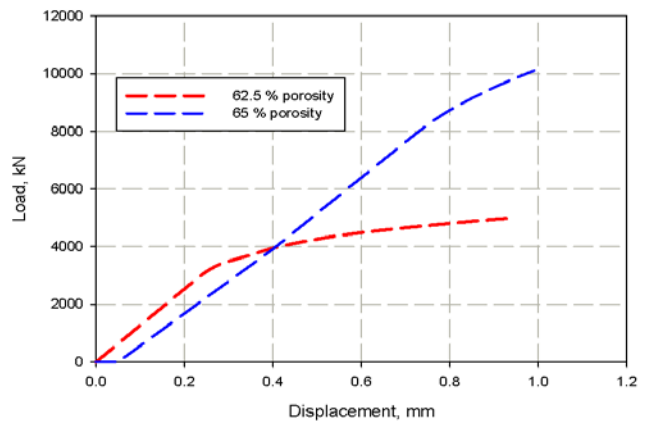


Figure 7. Predicted load-displacement relation for three-point single notch bending

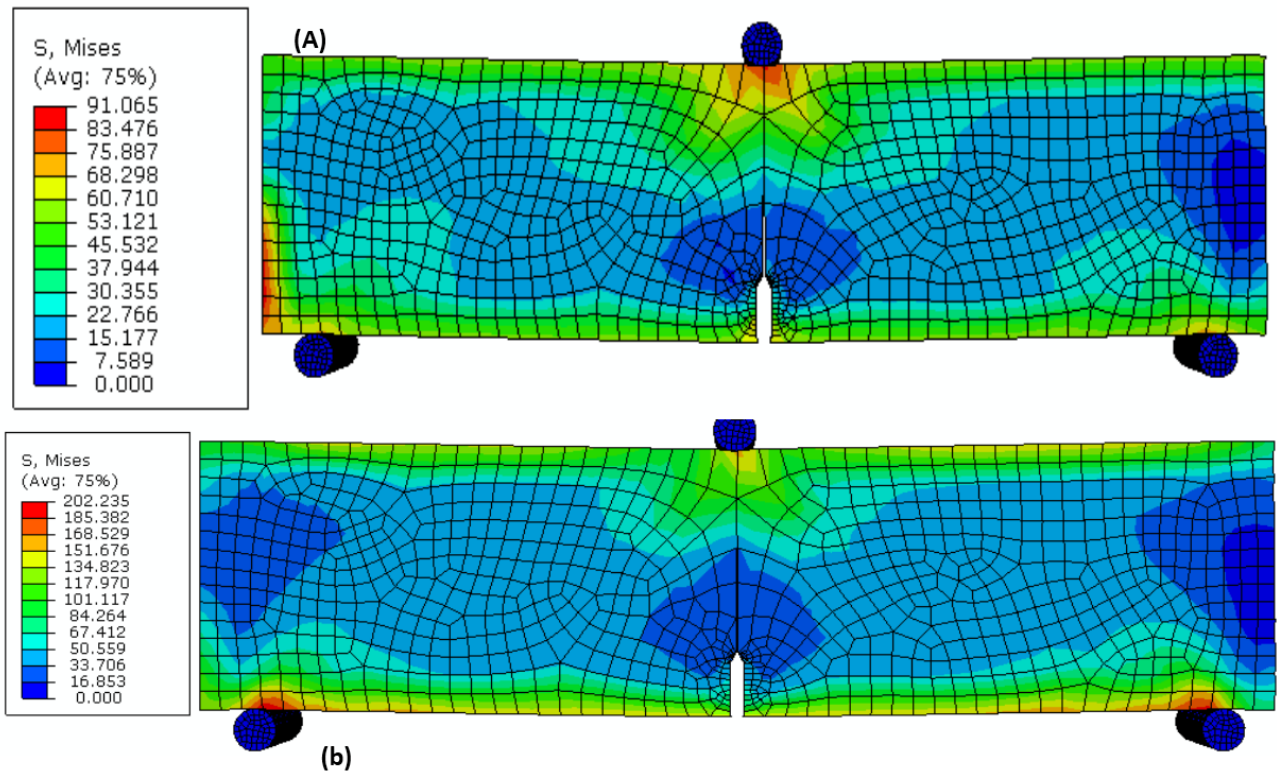


Figure 8. Mises stress for titanium foam A) 62.5 % b) 65 %

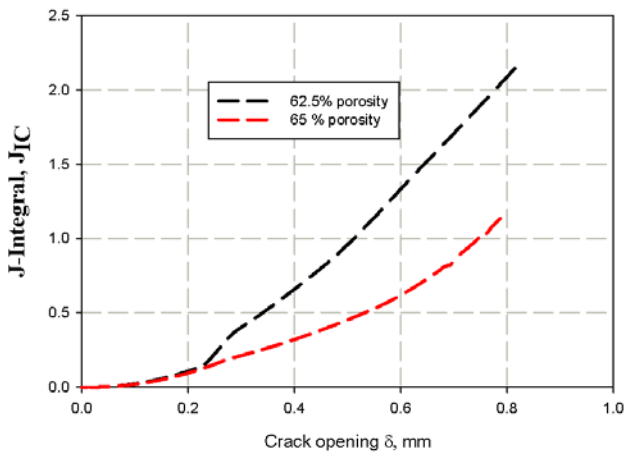


Figure 9. J-integral displacement relation for titanium foam

### 3. Conclusion

It is achieved the finite element model to measure the fracture toughness of titanium foam for use in human implants. The J-integral method is acceptable in case of linear material behavior like foams and it is assumed to be equal to surface release energy of mode I  $G_{IC}$ . This important fracture mechanics and the material characteristic parameter is well measured numerically and found to be (2.3), and (1.36)  $\text{kJ/m}^2$ , for 62.5% and 65 % porosity respectively Also, the model predicts well the three-point bending test load displacement.

### References

- [1] L.J. Vendra and A. Rabiei, "Evaluation of modulus of elasticity of composite metal foams by experimental and numerical techniques," *Mat. Sci. Eng.* Vol 527, pp. 1784-1790, 2007.
- [2] N. Tuncer and G. Arslan, "Designing compressive properties of titanium foams," *J. Mater. Sci.* vol 44, pp. 1477-1484, 2009.
- [3] J. Banhart, "Manufacture characterisation and application of cellular metals and metal foams," *Progress in Materials Science*, pp. 559-632, 2001.
- [4] M.F. Ashby, A.G. Evan, N.A. Fleck, L.J. Gibson, J.W. Hutchinson, H.N.G. Wadley, *Metal Foams: A Design Guide*. London: Butterworth-Heinemann, 2000.
- [5] M.I. Z. Ridzwan and S. Shuib, "Problem of stress shielding and improvement to the hip implant designs," *J. Med. Sci.* vol 4, pp. 460-467, 2007.
- [6] W. Yan and C.L. Pun, "Spherical indentation of metallic foams," *Mater. Sci. Eng. A*, vol 527, pp. 3166-3175, 2010.
- [7] A. Merdji, B. Bouiadjra, T. Achour, B. Seier, B. O. Chikh, and Z.O. Feng, "Stress analysis in dental prosthesis," *Com. Mater. Sci.*, vol 49, pp. 126-133, 2010.
- [8] J. Yang and HJ. Xiang, "A three-dimensional finite element study onthe biomechanical behaviour of an FGBM dental implant in surrounding bone," *J. Biomech.*, vol 40, pp. 2377-2385, 2007.
- [9] O. Kayabasi, E. Yuzbasioglu, and F. Erzincanli, "Static, dynamic and fatigue behaviors of dental implant using finite element method," *Adv. Eng. Soft.* Vol 37, pp. 649-658, 2006.
- [10] N. Djebbar, B. Serier, B. B. Bouiadjra, S. Benbarek, and A. Draï, "Analysis of the effect of load direction on the stress distribution in the dental implant," *Mater. Des.*, vol 31, pp. 2097-2101, 2010.
- [11] H. Schiefer, M. Bram, H.P. Buchkremer, and D. Stover, "Mechanical examinations on dental implants with porous titanium coating," *J. Mater. Sci: Mater. Med.*, vol 20, pp. 1763-1770, 2009.
- [12] W. Tanwongwan, J. Carmai "Finite Element Modeling of Titanium Foam Behavior for Dental Application" Proceedings of the World Congress on Engineering 2011 Vol III WCE 2011, July 6 - 8, 2011, London, U.
- [13] N. S. Korim, M. Y. Abdellah, M. Dewidar, and A.M. Abdelhaleem, "Crushable Finite Element Modeling of Mechanical Properties of Titanium Foam," *International Journal of Scientific & Engineering Research*, Vol. 6, Issue 10, pp. 1221-1227, October 2015.
- [14] T. Imwinkelried, T. "Mechanical properties of open-pore titanium foam," *J. Biomed Mater Res A*, pp. 964-970, 2007.
- [15] S. Kashef, A. Asgari, T. B. Hilditch, W. Yan, V. K. Goel, and P. Hodgson, "Fracture toughness of titanium foams for medical applications," *Mater. Sci. Eng. A*, vol 527, pp. 7689-7693, 2010.
- [16] H.L Schreyer, Q.H Zuo, A.K Maji, "Anisotropic plasticity model for foams and honeycombs" *J. Eng. Mech.* pp. 1913-1930, 1994.
- [17] R. Miller, "A continuum plasticity model of the constitutive and indentation behavior of foamed metals," *Inter. J. Mech. Sci.* pp. 729-754, 1999.
- [18] A. Nouri, A.B. Chen, P.D. Hodgson, and C.E. Wen, "Preparation and characterization of New Titanium Based Alloys for Orthopaedic and Dental applications," *Adv. Mater. Res.*, vol 15-17, pp.71-76, 2007.
- [19] J. Bin, W. Zejun, and Z. Naiqin, "Effect of pore size and relative density on the mechanical properties of open cell aluminium foams," *Scripta. Mater.*, vol 56, pp.169-172, 2007.
- [20] A.-F. Bastawros, H. Bart-Smith, and A.G. Evans, "Experimental analysis of deformation mechanisms in a closed-cell aluminum alloy foam," *J. Mech. Phys. Solids.*, vol 48, pp. 301-322, 2000.
- [21] L.J. Gibson and M.F. Ashby. *Cellular Solids: Structure and Properties*. 2nd ed. 1997, Cambridge University Press.
- [22] Mohammed Y. Abdellah, H. I. Fathi, A. M. M. Abdelhaleem, and M. Dewidar, "Mechanical Properties and Wear Behavior of a Novel Composite of Acrylonitrile-Butadiene-Styrene Strengthened by Short Basalt Fiber," *J. Compos. Sci.*, vol. 2, 2018.
- [23] M. K. Hassan, M. Y. Abdellah, A. F. Mohamed, T. S. ElAbiadi, S. Azam, and W. Marzouk, "Fracture Toughness of Copper/Glass-Reinforced Epoxy Laminate Composites," *American Journal of Materials Engineering and Technology*, vol. 6, pp. 1-7, 2018.
- [24] M. Y. Abdellah, "Comparative Study on Prediction of Fracture Toughness of CFRP Laminates from Size Effect Law of Open Hole Specimen Using Cohesive Zone Model," *Engineering Fracture Mechanics*, vol. 187, 2018.
- [25] M. Q. K. Mohammed Y. Abdellah, Mohammad S. Alsoufi, Nouby M. Ghazaly, G. T. Abdel-Jaber, "Mechanical Properties of Lab Joint Composite Structure of Glass Fiber Reinforced Polymers," *Materials Sciences and Applications*, vol. 8, pp. 553-565, 2017
- [26] M. Y. Abdellah, "Delamination Modeling of Double Cantilever Beam of Unidirectional Composite Laminates," *Failure analysis and prevention*, 2017.
- [27] Y. Mohammed, M. K. Hassan, H. El-Ainin, and A. Hashem, "Effect of stacking sequence and geometric scaling on the brittleness number of glass fiber composite laminate with stress raiser," *Science and Engineering of Composite Materials*, vol. 21, pp. 281-288, 2014.
- [28] M. Y. Abdellah, M. K. Hassan, T. Mandourah, and A. F. Mohamed, "Bearing Strength and Failure Behavior of Bolted GLARE Joints," *International Journal of Mechanical & Mechatronics Engineering IJMME-IJENS*, vol. 16, 2016.
- [29] N. S. Korim, Montasser Dewidar, Mohammed Y. Abdellah, Ayman M.M. Abdelhaleem, "Finite element modeling of mechanical properties of titanium foam and dental application," in *The third international conference on energy engineering (ICEE)*, 2015.
- [30] K. H. Mohamed, Y. A. Mohammed, S. Azabi, K., and W. W. Marzouk, "Investigation of the Mechanical Behavior of Novel Fiber Metal Laminates," *International Journal of Mechanical & Mechatronics Engineering IJMME-IJENS*, vol. 15, pp. 112-118, 2015.
- [31] Obert, R. et al. *Frictional Properties of BIOFOAM™ Porous Titanium Foam*. Wright Medical Technology, 5677 Airline Rd, Arlington, TN 38002.
- [32] ABAQUS 6.9 help, 2009.